

1
2
3
4
5
6
7 Detecting the genesis of a high performance carbon
8
9
10
11 supported Pd sulfide nano-phase and its evolution in
12
13
14
15
16 the hydrogenation of butadiene
17
18
19
20

21 *Belén Bachiller-Baeza,^a Ana Iglesias-Juez,^a Eva Castillejos-López,^b Antonio Guerrero-Ruiz,^{*b}*

22
23 *Marco Di Michiel,^c Marcos Fernández-García^a and I. Rodríguez-Ramos ^{*a}*
24
25

26
27 ^a Instituto de Catálisis y Petroleoquímica, CSIC, C/Marie Curie 2, 28049 Madrid (Spain).
28
29

30 ^b Departamento de Química Inorgánica y Química Técnica, UNED, C/ Senda del Rey 9, 28040
31
32 Madrid (Spain).
33
34

35
36 ^c ESRF, 6 Rue Jules Horowitz, 38043 Grenoble (France).
37
38
39
40
41
42

43 ABSTRACT. New procedure for preparation of palladium sulfide nanoparticles, which are
44 deposited-anchored over highly graphitized carbon nanofibers, is presented. The preparation
45 method is based in the use of PdSO₄ as metal precursor or alternatively in the previous
46 functionalization of the carbon surfaces with sulfonic groups by treatment with fuming sulfuric
47 acid. Using “in situ” high-energy X-ray diffraction technique, in both cases is demonstrated that
48 during the reduction treatment the initially present palladium hydride is transformed into a
49 palladium sulfide (Pd₄S). The catalytic properties of these materials have been tested in the gas
50
51
52
53
54
55
56
57
58
59
60

1
2
3 phase butadiene partial reduction to butenes. While metallic palladium nanoparticles supported
4
5 in the same carbon fibers produce butane as principal product, the supported Pd₄S nanocrystals
6
7 mainly yield different isomers of butenes independently of the conversion level. Furthermore
8
9 applying the same X-ray diffraction method is revealed that this catalytic phase is stable during
10
11 reaction.
12
13

14
15
16
17 KEYWORDS: catalyst synthesis, palladium sulfide, X-ray diffraction, hydrogenation reaction,
18
19 structure-activity relationship.
20
21
22
23

24 25 1. INTRODUCTION 26 27

28 Partial hydrogenation of alkynes and alkadienes in the presence of alkenes is one of the most
29
30 important processes in the chemical industry and selectivity is a relevant issue.¹ Supported
31
32 palladium catalysts are currently used for the hydrogenation of 1,3-butadiene, but because they
33
34 lack selectivity to the desired n-butenes when the ratio of monoalkenes to dienes is high,
35
36 promoters (Ag, Au, Ga or Cu) or modifiers (CO or sulfur) are needed to enhance the yield of
37
38 partially hydrogenated products.^{2, 3, 4, 5, 6} The reaction is known to be structure-sensitive^{7, 8} and it
39
40 has been reported that Pd catalysts under reaction can accommodate carbon atoms in subsurface
41
42 layers that affect the hydrogen diffusion improving the alkene selectivity.⁹
43
44
45

46
47 The use of carbon materials as supports of metal nanoparticles is widely employed for
48
49 preparing heterogeneous catalysts, among others because as consequence of the moderate metal-
50
51 graphite interaction new chemical compositions can be easily synthesized, i.e. intermetallic
52
53 compounds⁵ or transition metal sulphides.¹⁰ In addition, modification of carbon surface with
54
55 functionalities has been used for anchoring metal nanoparticles to the carbon surface.^{11,12}
56
57
58
59
60

1
2
3 Supported palladium sulfides catalysts are generally synthesized through pre-sulfidation of
4 supported Pd metal catalysts using H₂S, Na₂S or organic sulfur-containing molecules,^{10,13} but
5 such methods have the problems of high environmental pollution and scaling cost.^{1,3} Recently,
6 thiolate self-assembled monolayers were used to block specific active sites on Pd/Al₂O₃ during
7 the hydrogenation of furfural.¹⁴ The adsorbed thiolate modifiers serve the role of isolating certain
8 highly active sites for hydrodeoxygenation reaction, restricting selectivity toward undesired
9 products. Moreover, preformed palladium sulfide nanoparticles grafted on graphene oxide (GO)
10 have been reported for catalysis of the Suzuki coupling reaction.¹⁵ In this latter case, the Pd
11 sulfide nanoparticles were prepared by thermolysis of an organometallic precursor containing
12 Pd-S bonds. This method reduces the toxicity risks and contamination. However, the palladium
13 sulfide/GO composite suffers significant leaching of the active Pd during the catalytic reaction
14 what hinders its recyclability. Therefore, it seems necessary to develop new simple and safe
15 methods to synthesize supported palladium catalysts and obtain more detailed insight into their
16 evolution and stability under reaction conditions.
17
18
19
20
21
22
23
24
25
26
27
28
29
30
31
32
33
34
35
36

37 Herein, we present a study showing the formation and the evolution under reaction conditions
38 of Pd sulfide nanoparticles supported on carbon nanofibers by coupling time resolved high-
39 energy X-ray diffraction (HEXRD) and mass spectrometry (MS). This approach allows us to
40 simultaneously investigate in a time resolved manner the structure–activity relationship of the
41 supported Pd nanoparticles, and the compounds that are formed or converted over them.¹⁶ We
42 characterize the nature of the Pd-based nanoparticles generated by reduction under hydrogen
43 flow at 250 °C of two metal precursors, Pd chloride and Pd sulfate, deposited (1wt% of Pd) on
44 carbon nanofibers functionalized with sulfonic or carboxylic groups, respectively. Also, we study
45 the evolution of these Pd based catalysts under butadiene hydrogenation reaction conditions.
46
47
48
49
50
51
52
53
54
55
56
57
58
59
60

2. EXPERIMENTAL SECTION

Preparation of carbon supports. A commercial carbon nanofibers was used in this study: Pyrograph III PR24-HHT (SBET = 32 m²/g) provided by Applied Sciences Inc. The PR24-HHT fibers (denoted as HHT) was originally treated at high temperature (~3030 °C), possess a stacked-cup morphology with a hollow core through the length of the fiber and also present a jagged outer surface with “round heads” or “loop” structures which connect several layers.¹⁷

HHT was functionalized according to reported procedures yielding HHTox.¹⁸ Briefly, parent carbon nanofiber was refluxed in 50% nitric acid (carbon/HNO₃ = 1 g/10 mL) at 100 °C for 48 h in order to increase the concentration of functional groups on the surface. HHT was also subjected to a sulfonation treatment.¹⁹ Aliquots of 3 g of fibers were immersed in 150 mL of fuming sulfuric acid (15 wt % SO₃) at 80 °C under a nitrogen gas atmosphere for 7 h. After the treatment, the suspension was washed with deionized water to remove any excess sulfuric acid in the carbon nanomaterial, filtered and dried at 120 °C. The resulting modified sample was labelled HHT-SO₃H. Elemental chemical analysis of carbon, hydrogen and sulfur was carried out in a LECO CHNS-932 instrument. The results reveal a 1wt% content of sulfur.

Catalyst preparation. Catalysts were prepared by incipient wetness impregnation of the supports with water solutions of PdCl₂ or PdSO₄. The catalysts were prepared with a 1 wt% Pd loading. In the case of PdCl₂, the precursor was dissolved in concentrated HCl to generate tetrachloride palladium acid (H₂PdCl₄), heated to eliminate chlorine, dissolved in distilled water, dried and again diluted in water until the final volume was reached. This solution was dropped to the carbon nanofiber supports (HHTox and HHT-SO₃H).

1
2
3 **Characterization details.** The chemical nature of the functional groups of the two supports
4 was evaluated by temperature programmed desorption coupled with mass spectrometer (TPD-MS)
5 experiments under vacuum in a conventional volumetric apparatus connected to a RGA-200 SRS
6 mass spectrometer.²⁰ The sample was evacuated for 30 min at room temperature and then
7 ramped to 1023 K at a 10 K min⁻¹ rate.
8
9

10
11
12
13
14
15
16 All the samples were characterized by X-ray photoelectron spectroscopy (XPS),
17 thermogravimetry and transmission electron microscopy (TEM) analyses. X-ray photoelectron
18 spectra of the supports and catalysts were recorded with an ESCA-PROBE P (Omicron)
19 spectrometer by using non-monochromatized Mg-K α radiation (1253.6 eV). The binding energy
20 of Pd 3d and S 2p were internal referenced to the C 1s line at 284.6 eV. The error in
21 determination of electron binding energies did not exceed 0.2 eV. Each sample was pressed into
22 a small pellet of 15 mm diameter and placed in the sample holder and degassed in the chamber
23 for 6-8 h to achieve a dynamic vacuum below 10⁻⁸ Pa before analysis. The spectral data for each
24 sample was analyzed using CASA XPS software. The relative concentrations and atomic ratios
25 were determined from the integrated intensities of photoelectron lines corrected for the
26 corresponding atomic sensitivity factor.
27
28
29
30
31
32
33
34
35
36
37
38
39
40
41
42

43 Transmission electron microscopy (TEM) images of the catalysts were measured using a JEOL
44 JEM-2100 field-emission gun electron microscope operated at 200 kV. The samples were
45 ground, ultrasonically suspended in ethanol and then dripped onto a carbon-coated copper grid
46 before TEM images were generated. The mean diameter (d) of the Pd particle size were
47 calculated based on a minimum of 100 particles.
48
49
50
51
52
53
54
55
56
57
58
59
60

1
2
3 High-energy X-ray diffraction (HEXRD) data were collected at the ID15A beamline at the
4 ESRF-The European Synchrotron with a wavelength of 0.17750 Å (69.85 KeV), using a Perkin
5 Elmer area detector and a sample-detector distance of 650 mm. The diffraction patterns were
6 collected with an exposure time of 30 seconds. Diffraction data were fitted using the Rietveld
7 method with the XPert Highscore Plus program (Panalytical). The reactor and heat gun were
8 mounted on a Huber stage capable of translations in the x, y and z directions. The carbon fibres
9 supported catalysts were pressed into pellets and sieved to a size of 0.075 to 0.150 mm. Aliquots
10 of these pellet samples were loaded in a fixed bed quartz tube of 2 mm internal diameter, located
11 between two glass wools. The flow of reaction gases feed to the reactor was constant at 20
12 ml·min⁻¹, with compositions of 15% hydrogen in helium during temperature programmed
13 reduction experiments and 15% hydrogen+3% butadiene in helium during hydrogenation
14 reaction conditions. H₂/H₂+Bd/H₂ alternate exposures at constant increasing temperatures were
15 applied with an exposure time of 30 min for each atmosphere. The reactor was heated with one
16 Leister LE mini heat gun fitted with a heat spreader. The temperature inside the catalytic bed was
17 measured using a thermocouple inserted into the carbon supported sample. The range of
18 operation temperatures was from room temperature up to 550 K. The exhaust products from the
19 reactor were analyzed using a European Spectrometry ecoSyst-P Man-Portable mass
20 spectrometer with capillary inlet and heated inlet tubes.
21
22
23
24
25
26
27
28
29
30
31
32
33
34
35
36
37
38
39
40
41
42
43
44
45

46
47 **Catalytic measurements.** Steady state catalytic experiments for butadiene (Bd) hydrogenation
48 were carried out in a continuous flow fixed-bed reactor (4 mm inner diameter). Before reaction,
49 the catalyst was pretreated in flowing H₂ at 250 °C for 1 h. The reactants H₂ (10% vol) and Bd (2
50 % vol) with the balance of N₂ passed through the catalyst bed at a total flow rate of 60 mL/min.
51 The hydrogen amount was in large excess. Any significant mass-transfer limitation was
52
53
54
55
56
57
58
59
60

1
2
3 precluded by using this high linear velocity and powder (sieve fraction 150-250 μm) catalysts.
4
5 The occurrence of external diffusion limitations was ruled out by running tests where both the
6
7 flow rate and the catalyst amount were significantly changed while keeping the mass/flow rate
8
9 ratio constant ($8.3 \cdot 10^{-6}$ g·h/ml). The reaction temperature was varied between room temperature
10
11 and 473 K at atmospheric pressure. The reactor effluent was on-line analyzed using a gas Varian
12
13 3400 gas chromatograph with flame ion detector (FID) and thermal conductivity detector (TDC)
14
15 with a 20% BMEA Chromosorb P80/100 column.
16
17
18
19
20
21
22
23

24 3. RESULTS AND DISCUSSION

25
26
27 Table 1 summarizes the performance of the $\text{PdCl}_2\text{-HHT-SO}_3\text{H}$ and $\text{PdSO}_4\text{-HHTox}$ catalysts in
28
29 the selective hydrogenation of butadiene (Bd) obtained in a fixed bed reactor with the reaction
30
31 mixture of $\text{H}_2\text{:Bd:N}_2$ of 10:2:88. The $\text{PdCl}_2\text{-HHTox}$ sample is included as a reference for
32
33 comparison. This latter catalyst displays high activity (100% conversion of butadiene is reached
34
35 at room temperature) but is totally unselective to partial hydrogenation, as butane was the only
36
37 product. However, when sulfur is initially present in the catalyst precursor, either as surface
38
39 sulfonic groups on the support or as moieties coming from the Pd precursor, the reduced catalyst
40
41 (250 $^\circ\text{C}$ -2h in hydrogen) shows high selectivity for the hydrogenation of butadiene to butenes
42
43 (99% of butenes in the case of $\text{PdSO}_4\text{-HHTox}$ at 100% conversion) although the activity is
44
45 somewhat reduced as the selectivity increases from $\text{PdCl}_2\text{-HHT-SO}_3\text{H}$ to $\text{PdSO}_4\text{-HHTox}$.
46
47 Clearly, the presence of the sulfur modifier has to be related with the selective performance of
48
49 the $\text{PdCl}_2\text{-HHT-SO}_3\text{H}$ and $\text{PdSO}_4\text{-HHTox}$ catalysts, in special in the last case. Such marked
50
51 changes in selectivity require further investigation.
52
53
54
55
56
57
58
59
60

Table 1. Results characterizing the performance of Pd catalysts in the selective hydrogenation of butadiene.^a

Sample	T ₃₀ (°C)	T ₁₀₀ (°C)	S ₃₀ (%)	S ₁₀₀ (%)
PdCl ₂ -HHTox	-	25	0	0
PdSO ₄ -HHTox	120	150	99	99
PdCl ₂ -HHT-SO ₃ H	100	120	99	75

^a T₃₀ and T₁₀₀, temperature at which the 30% and 100% conversion of butadiene is achieved. S₃₀ and S₁₀₀, selectivity toward partial hydrogenation at 30% and 100% conversion. Reaction performed in a fixed bed reactor with the reaction mixture of H₂:Bd:N₂ of 10:2:88, 30 mg catalyst.

Figure 1 presents the HRTEM pictures and histograms with the size distribution of palladium particle diameters for the different catalysts reduced at 250 °C. A broad range of particle sizes and a relative regular distribution of the Pd particles over the support are observed for the distinct catalysts. Both features can arise from the high graphitization degree and low defect density produced by surface functionalization of the support. However, the particle size distribution is shifted towards smaller sizes for the catalysts containing sulfur in the catalyst precursor. Thus, between 65-75% of the metallic particles in PdSO₄-HHTox and PdCl₂-HHT-SO₃H catalysts have diameters below 4 nm. The micrographs (Figure 1 and Figures S2-S4 in supplementary information) show the spherical nature of the Pd particles for the different catalysts, particularly for the PdCl₂-HHTox, which, as said, could be consequence of a weak interaction between the particles and the nanofibers.

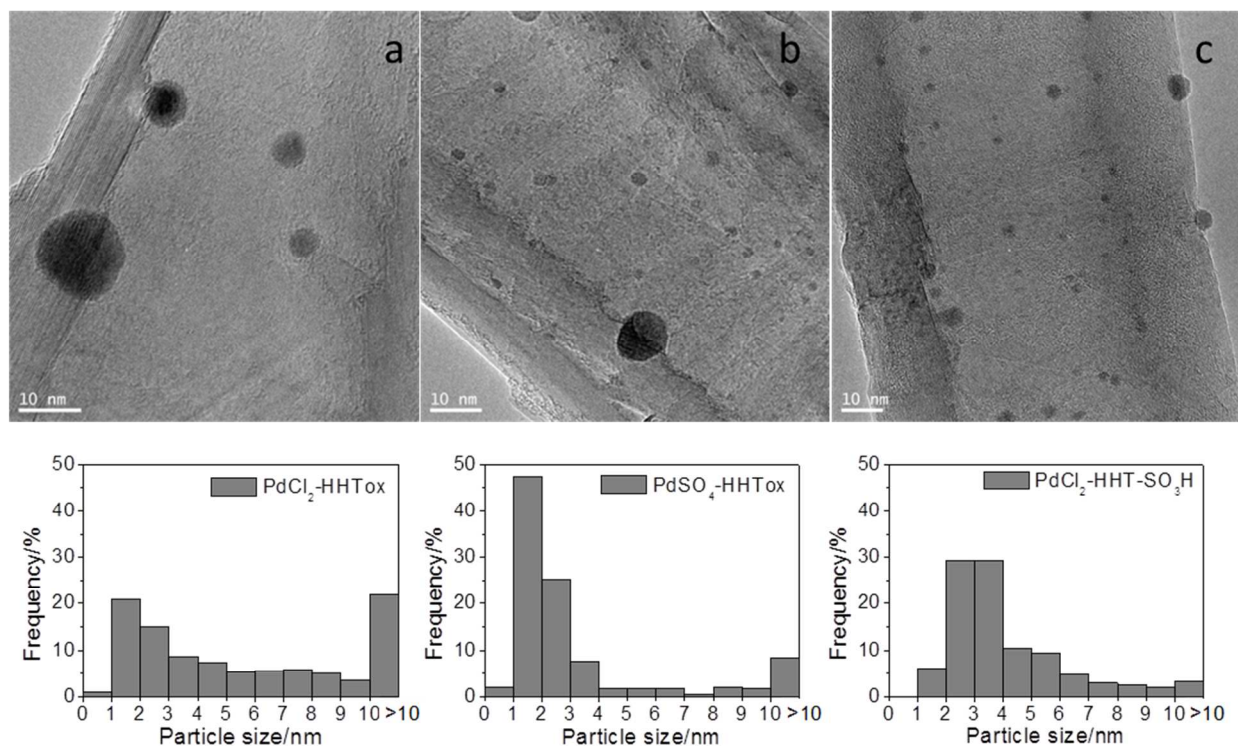


Figure 1. HRTEM micrographs and histograms with the size distribution of particle diameters for a) PdCl₂-HHTox, b) PdSO₄-HHTox and c) PdCl₂-HHT-SO₃H catalysts reduced at 250 °C.

The mean particle diameters (d) of Pd calculated from TEM measurements of the different samples are displayed in Table 2. The mean volume particle diameters ($d_{4/3}$) were also estimated and included in Table 2. The mean volume particle diameter, sensitive to the volume of particles, gives more weight to the larger particles and is more appropriate than mean particle size for comparison with data obtained from physical techniques such as X-ray line broadening or magnetic methods.

Table 2. Mean particle size (d) and volume-surface mean particle size ($d_{4/3}$) estimated from TEM measurements.

Catalyst	$\Sigma n_i d_i / \Sigma n_i$ (nm)	$\Sigma n_i d_i^4 / \Sigma n_i d_i^3$ (nm)
PdCl ₂ -HHTox	6.6	18.3
PdSO ₄ -HHTox	4.6	17.1
PdCl ₂ -HHT-SO ₃ H	4.2	8.5

Characterization under realistic reaction conditions of supported nanoparticles with spread size-distribution of Pd nanoparticles and mean size around 4.5 nm (from TEM measurements) is not an easy task since no so many methods can be applied to this type of materials. Conventional X-ray diffraction techniques (XRD) performed at laboratory diffractometer provide non useful information on low loading metal supported catalysts as due to the low signal intensity. In contrast, using synchrotron-based radiation the high energy X-ray diffraction (HEXRD) can provide structural information on finely dispersed palladium on catalysts under reaction conditions. Physical methods, such as high resolution transmission electron microscopy (HRTEM), fail when these nanoparticles have to be studied in situ in a catalyzed reaction, in fact HRTEM measurements should be performed under high vacuum conditions, moreover statistical measurements of microdiffraction over a large number of particles are difficult to achieve.

To investigate the nature of the Pd-based nanoparticles in the different catalysts during the temperature programmed reduction in hydrogen we use HEXRD coupled with MS. Color map representation in Figure 2 shows the variation of the HEXRD patterns for the Pd catalysts from room temperature to 250 °C.

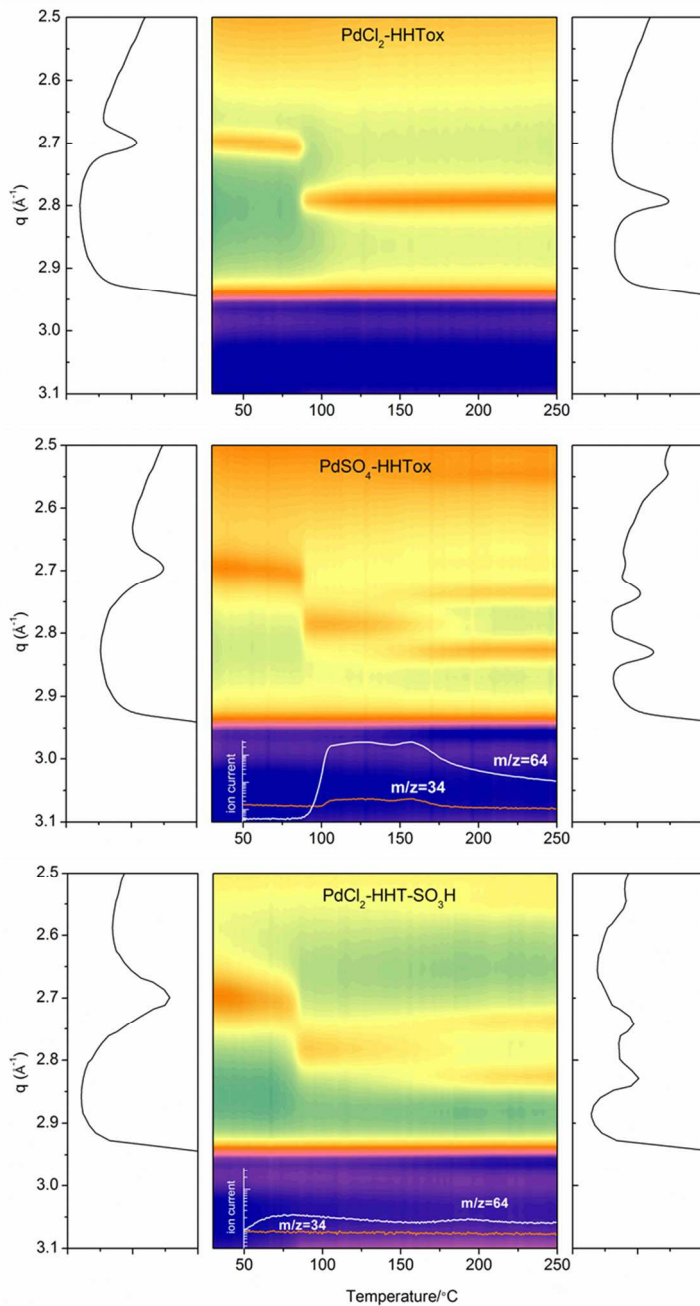


Figure 2. Intensity contour maps of the HEXRD patterns obtained during temperature programmed reduction in hydrogen/helium from room temperature up to 250 $^{\circ}\text{C}$. Initial and final HEXRD patterns are showed on the left and right of panels, respectively. MS ($m/z = 34$ and 64) analysis of gases evolved during the heating treatment is showed in the blue graph insets.

1
2
3 When the PdCl₂-HHTox sample (upper panel) is exposed to hydrogen/helium at room
4 temperature the HERXD pattern reveals the formation of the β phase of Pd hydride (peak (111)
5 at 2.70 Å⁻¹).²¹ Heating to higher temperature it is seen that above 90°C the most intense (111)
6 reflection shifts to higher Q value (2.80 Å⁻¹) due to the lattice contraction as hydrogen is released
7 from the hydride phase to form metallic Pd (lattice constant at 250 °C, a= 3.904 Å).
8
9

10
11 The structural evolution of the sample prepared with palladium sulfate (PdSO₄-HHTox, middle
12 panel) is different after the transformation into metallic Pd at 90 °C because as the temperature
13 approaches the 150 °C a second transformation occurs, resulting in the formation of the Pd₄S
14 phase ((210) and (112) peaks at 2.74 and 2.83 Å⁻¹, respectively).²² The formation of the Pd
15 sulfide phase is further described with the help of MS. In Figure 2 as an inset onto color maps
16 selected MS signals labelled m/z = 34 and m/z = 64 are plotted. The first one is associated to H₂S
17 while the m/z = 64 corresponds to SO₂. Both products stem as main gas residues coming from
18 the decomposition/reduction of the sulfate anions of the metal precursor deposited on the support
19 and appear with a constant level from 100 to 160 °C. At this latter temperature Pd is completely
20 transformed to the single well crystalized Pd₄S structure (lattice constants at 250 °C, a= 5.137 Å,
21 c = 5.623 Å). Although sulfidation of supported metallic palladium with H₂S or Na₂S usually
22 leads to mixed crystal phases, formation of a single phase seems to be favored when Pd is
23 supported on carbon.¹⁰ The formation of palladium sulfides supported on carbon is highly
24 dependent on the composition of the sulfidation atmosphere and temperature. Single phase of
25 Pd₄S was reported at 150°C under H₂S/H₂ ratios between 0.008 and 0.25.^{10,23}
26
27
28
29
30
31
32
33
34
35
36
37
38
39
40
41
42
43
44
45
46
47
48
49

50 In the case of the PdCl₂-HHT-SO₃H (lower panel), the complete transformation of β phase of
51 Pd hydride to Pd is observed at 90°C. From 150 °C and above up to 250 °C only part of the Pd
52 metal is transformed to Pd₄S (lattice constants, a = 5.136 Å, c = 5.619 Å). The presence of a
53
54
55
56
57
58
59
60

1
2
3 minor metallic Pd phase is successfully tracked out in the high resolution XRD patterns
4 presented in Figure 2 (bottom). HEXRD fitting using the Rietveld method reveals that a 21 wt%
5 of metallic Pd remains (see Supporting Information, Table S1). From the MS analysis (inset,
6 lower panel), we learn that the evolution of H₂S and SO₂ is appreciably lower than for the
7 PdSO₄-HHTox sample and clearly not enough to transform the whole metallic Pd into Pd₄S. Both
8 fresh samples, PdSO₄-HHTox and PdCl₂-HHT-SO₃H, have similar initial sulfur content, 1wt%
9 SO₄⁻ and 1wt% SO₃H, respectively.
10
11
12
13
14
15
16
17
18

19
20 Surface chemical analysis by XPS of fresh samples clearly evidenced the presence of sulfur on
21 the surface, since the characteristic peak stemming from the overlapped S 2p_{3/2} and S 2p_{1/2}
22 doublet (spin-orbit splitting of 1.2 eV, see Figure S7 in supporting information) was revealed at
23 around 169 eV which is characteristic of sulfate (Figure 3) and -SO₃H groups (result not shown).
24 After reduction at 250 °C, the XPS spectra show that the PdCl₂-HHT-SO₃H sample still has
25 sulfonic groups on the surface while the surface of PdSO₄-HHTox sample is practically free of
26 sulfur. Moreover, no S 2p peaks emerging from sulfide or S_n species, expected at 161.5 and
27 163.5-164 eV respectively, were found.¹³
28
29
30
31
32
33
34
35
36
37
38
39
40
41
42
43
44
45
46
47
48
49
50
51
52
53
54
55
56
57
58
59
60

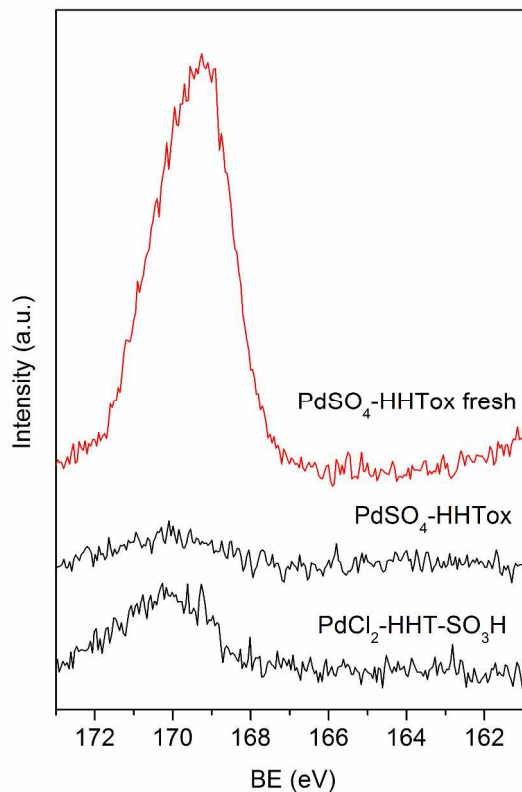
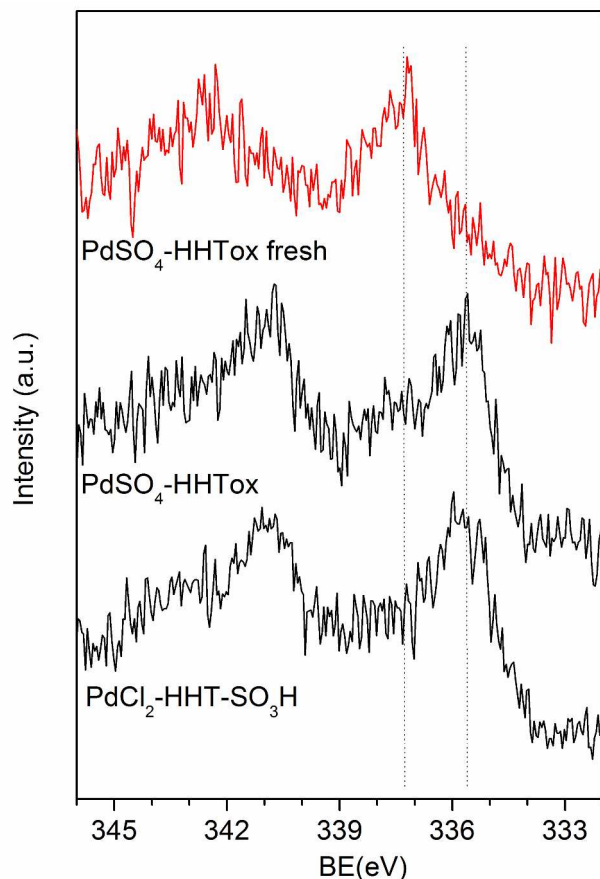


Figure 3. XPS spectra of the S 2p core level for the PdSO₄-HHTox and PdCl₂-HHT-SO₃H catalysts reduced at 250 °C and the fresh PdSO₄-HHTox.

The XPS spectra for the doublet Pd 3d_{5/2} and 3d_{3/2} of the fresh PdSO₄-HHTox and the PdSO₄-HHTox and PdCl₂-HHT-SO₃H catalysts reduced at 250 °C are shown in Figure 4. It is observed that the Pd 3d_{5/2} peak shifts from 337.3 eV (Pd²⁺ in the PdSO₄-HHTox sample) to 335.5 eV for the two reduced samples. This value of binding energy (Pd 3d_{5/2} at 335.5 eV) suggests that the oxidation state of Pd is zero in both reduced catalysts.^{5,24}



33 **Figure 4.** XPS spectra of the Pd 3d core level for the PdSO₄-HHTox and PdCl₂-HHT- SO₃H
34 catalysts reduced at 250 °C in hydrogen and the fresh PdSO₄-HHTox sample.
35
36

37
38
39 It is worth noting that our results are very close to those previously obtained in a study on non-
40 supported Pd₄S nanoparticles where a zero oxidation state for both Pd and S was found by XPS
41 measurements.¹⁵ In this latter work the possibility of charge transfer from Pd to S in Pd₄S is also
42 discussed based on a marginal shift of the Pd 3d binding energy with respect to that of pure Pd.
43 In our case the difference between the value of 335.5 eV for the Pd 3d_{5/2} in the reduced PdSO₄-
44 HHTox and PdCl₂-HHT- SO₃H catalysts and those found in the literature^{5,24} for Pd zero is of 0.2
45 eV as maximum, which is within the error of determination. Therefore, the XRD identified Pd₄S
46 phase may be described as an alloy type compound with structure basically similar to Pd⁰ where
47 the S atoms occupy substitutional sites resulting in some distortions. In addition, it has been
48
49
50
51
52
53
54
55
56
57
58
59
60

1
2
3 reported that Pd₄S can intrinsically behave as a metal, especially in relation to conducting
4 electrons.²⁵ The values of mean particle size estimated using Scherrer equation for the Pd₄S
5
6 phase are of 17.4 and 10.8 nm for PdSO₄-HHTox and PdCl₂-HHT-SO₃H catalysts reduced at 250
7
8 °C, respectively.
9
10

11
12 Figure 5 shows the evolution of Pd phases of reduced catalysts under butadiene
13 hydrogenation reaction atmosphere at different temperatures and during H₂/H₂+Bd/H₂
14 alternate exposure. Once the catalysts were treated in hydrogen at 250 °C the temperature
15 was cooled down to the corresponding reaction temperatures which were selected for
16 each catalyst within the range of activity shown in Table 1.
17
18
19
20
21
22
23
24
25
26
27
28
29
30
31
32
33
34
35
36
37
38
39
40
41
42
43
44
45
46
47
48
49
50
51
52
53
54
55
56
57
58
59
60

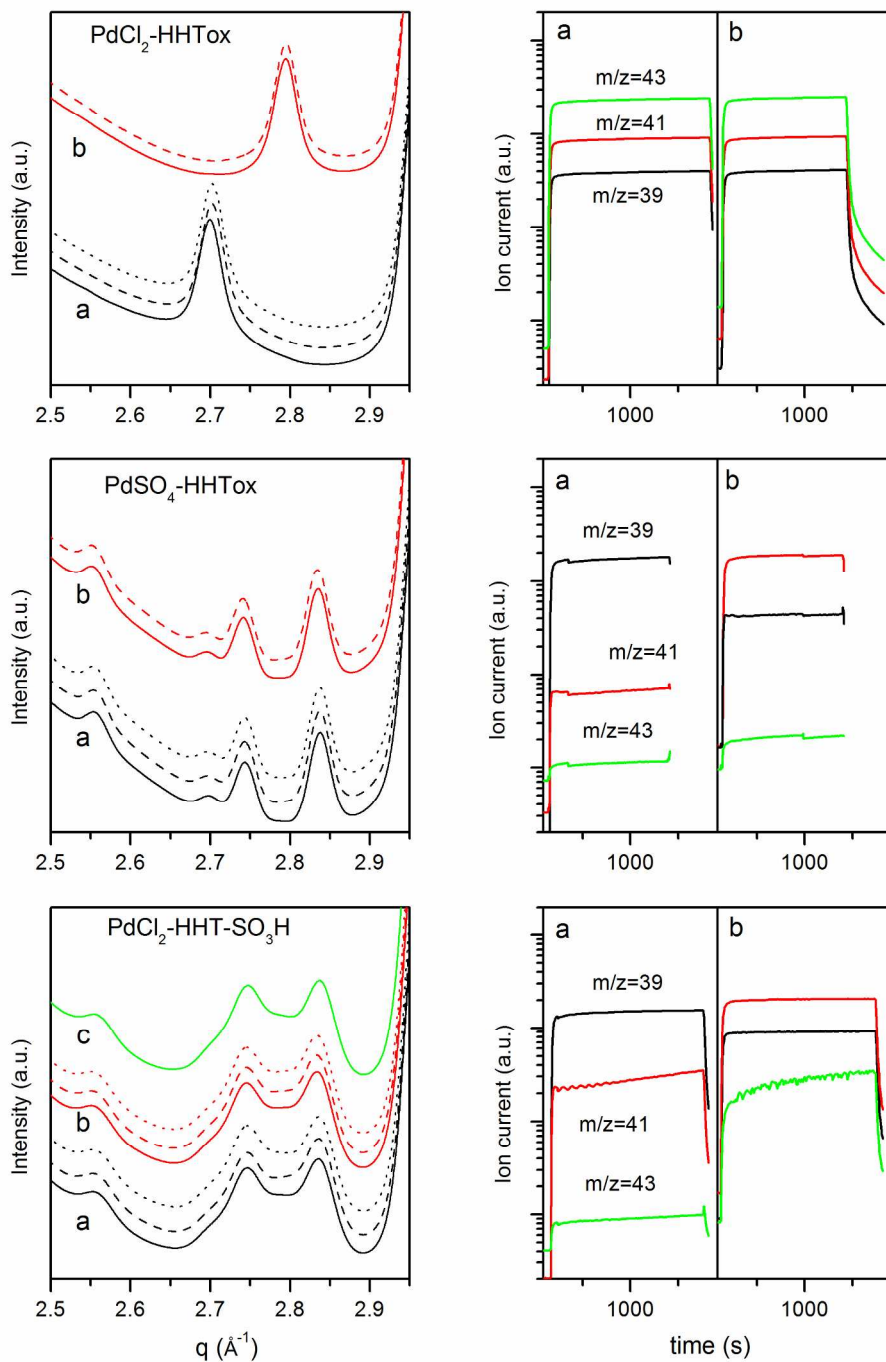


Figure 5. HEXRD patterns obtained under consecutive H₂ (—), H₂+Bd (- - -), H₂ (...) atmospheres at several constant temperatures and MS results for selected m/z values under H₂+Bd. Upper panels: $\text{PdCl}_2\text{-HHTox}$; a: RT, b: 150 °C. Middle panels: $\text{PdSO}_4\text{-HHTox}$; a: 100 °C, b: 160 °C. Lower panels: $\text{PdCl}_2\text{-HHT-SO}_3\text{H}$; a: 100 °C, b: 140 °C, c: RT.

1
2
3 The structural study of the reference PdCl₂-HHTox sample reveals at room temperature no
4 changes in the lattice parameters of the formed β-Pd hydride phase during the H₂/H₂+Bd/H₂
5 alternate exposure. The same applies for the Pd phase at 150 °C which remains unchanged under
6 the different atmospheres. MS analysis under H₂+Bd atmosphere confirms that both phases of
7 palladium (β-Pd hydride and metallic Pd) are active at the corresponding reaction temperatures.
8 In Figure 5 signals labelled m/z = 39, 41 and 43 are plotted. The first one is associated to the
9 reactant, butadiene, while the other two correspond to the reaction products butenes and butane,
10 respectively. It is observed the non-selective total hydrogenation of butadiene and major
11 production of butane. This PdCl₂-HHTox sample has not preferential growth of particles along a
12 given crystallographic direction and is made of spherical nanoparticles (see HRTEM
13 micrographs at Figure 1 and at Supporting Information, Figure S2), thus, it could be assumed
14 that exposes a major fraction of the most thermodynamically stable (111) surfaces. Earliest
15 comparative studies with different nanostructured Pd catalysts established that the (100) facets
16 are more active for the butadiene hydrogenation, but also more selective for ceasing the reaction
17 at the butenes than the (111) surfaces.^{26,27} Similarly, Silvestre et al.⁷ also observed that (110)
18 surfaces are particularly selective for the hydrogenation of dienes into alkenes. Moreover,
19 selective partial hydrogenation of dialkenes and alkynes to alkenes on Pd catalysts has been
20 related with the formation of sub-surface layers of Pd carbide (PdC_x) which limits the diffusion
21 of hydrogen and its availability for hydrogenation reaction.^{2,9} The isotropic palladium
22 nanoparticles and the absence of Pd carbide phase (detectable in our experimental conditions for
23 a chemical composition PdC_x, with x larger than 0.002)²⁸ in the PdCl₂-HHTox sample upon
24 exposition to the reaction atmosphere at both temperatures (RT and 150 °C) likely explain its
25 unselective catalytic behavior in the butadiene hydrogenation.
26
27
28
29
30
31
32
33
34
35
36
37
38
39
40
41
42
43
44
45
46
47
48
49
50
51
52
53
54
55
56
57
58
59
60

1
2
3 The same HEXRD study carried out over PdSO₄-HHTox sample reveals also no structural
4 changes in the phase formed during reduction in hydrogen at 250 °C (Figure 5). Thus, the lattice
5 parameters of the Pd₄S phase remains constant, with variations far below the estimated error of ±
6 0.004 Å, during the time of exposition to reaction mixture and switching to hydrogen at both 100
7 and 150 °C temperatures. In addition, the MS analysis shows, in agreement with the previous
8 steady state catalytic studies (Table 1), the high selectivity of the catalyst for the partial
9 hydrogenation of butadiene (m/z = 39) into butenes (m/z = 41). Theoretical investigations of H₂
10 dissociation on the faces of Pd₄S indicate that dissociation barriers are higher than on Pd (111)
11 face, although low enough to allow the partial hydrogenation of dialkenes and alkynes.²⁹
12 Therefore, the Pd₄S phase constitutes an active and selective catalytic phase for partial
13 hydrogenation of polyunsaturated hydrocarbons. Interestingly, the palladium sulfide phase is
14 stable during the H₂/H₂+Bd/H₂ alternate exposures whereby regeneration of the catalyst with
15 further feeding a sulfur compound, common practice in hydrorefining plants,^{1,3} is likely
16 unneeded. The stability of the Pd₄S phase in the PdSO₄-HHTox catalyst under reaction
17 conditions is also proved by a long term catalytic run performed in fixed bed reactor at 100 °C,
18 with 60 ml of the reaction mixture of H₂:Bd:N₂ (10:2:88) and 30 mg of catalyst (Figure 6). It can
19 be seen that activity and selectivity were maintained during the run.
20
21
22
23
24
25
26
27
28
29
30
31
32
33
34
35
36
37
38
39
40
41
42
43
44
45
46
47
48
49
50
51
52
53
54
55
56
57
58
59
60

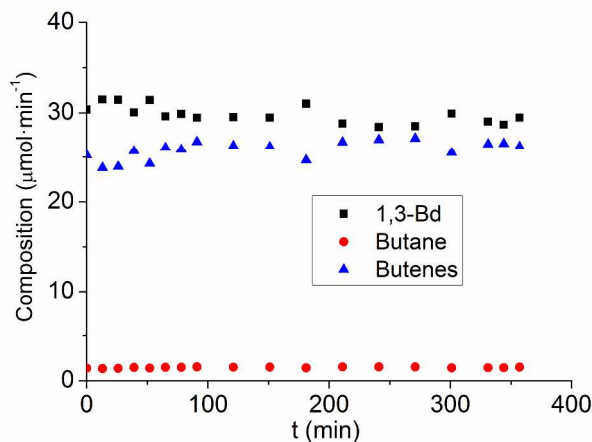


Figure 6. Stability test carried out at 100 °C on the PdSO₄-HHTox catalyst.

Similarly, in the case of PdCl₂-HHT-SO₃H sample (Figure 5 lower panels), the two phases (79% Pd₄S and 21% Pd) formed after reduction treatment remain unchanged upon H₂/H₂+Bd/H₂ alternate exposures at 100 and 140 °C. Strikingly, when the temperature is cooled down to room temperature in hydrogen atmosphere the foreseeable change in the Pd metal d spacing due to the β-Pd hydride phase formation does not occur. Likely, we have nanoparticles with a Pd@Pd₄S core-shell nanostructure where the Pd₄S shell hinders the diffusion of hydrogen to the Pd core. It is known H₂ permeability of Pd₄S is more than one order of magnitude lower than that of metallic Pd.³⁰

Considering the results of our temperature programmed reduction in hydrogen experiments where we used HEXRD coupled with MS experiments (Figure 2) and in agreement with the literature,³¹ we believe that the sulfidation process is a stepwise process which comprise (1) decomposition of H₂S and SO₂ precursors (sulfate anions and sulfonic groups for PdSO₄-HHTox and PdCl₂-HHT-SO₃H, respectively), (2) adsorption of these gaseous molecules on the surface of the metallic Pd nanoparticles initiating the sulfidation at the surface at around 150 °C and (3) finally progressing of sulphur into the bulk of Pd particles. Hence, the formation of bulk Pd₄S

1
2
3 nanoparticles in the reduced PdCl₂-HHT-SO₃H catalyst is likely precluded for the limited
4 decomposition, at temperatures below 250 °C, of the sulfonic groups covalently anchored to the
5 surface of the support (see Supporting information, Figure S1).
6
7
8
9

10 The MS analysis under reaction (Figure 5 lower panels) shows a high selectivity to partial
11 hydrogenation at 100 °C while at 140 °C some proportion of butane is produced. Moreover, this
12 PdCl₂-HHT-SO₃H sample, in agreement with catalytic studies (Table 1), is somewhat more
13 active than the PdSO₄-HHTox. The higher catalytic activity of the former can be clearly
14 attributed to the larger dispersion of the active Pd₄S phase. Moreover, the smaller particle size in
15 this sample turns into a higher proportion of unsaturated sites at edges and corners on where the
16 H₂ dissociation barrier becomes likely reduced and therefore the partial hydrogenation of
17 dialkenes deprived at higher reaction temperatures.^{2,29}
18
19
20
21
22
23
24
25
26
27
28

29 In summary, we have developed a simple and green method to produce an active, very stable
30 and highly selective catalyst for the butadiene hydrogenation (here named PdSO₄-HHTox) based
31 on the pure Pd₄S phase supported on carbon nanofibers. The palladium sulfide precursor is a
32 common palladium sulfate salt impregnated on the carbon support. The catalyst is produced in a
33 single step via reduction process in hydrogen atmosphere without further sulfidation.
34
35
36
37
38
39
40
41
42

43 4. CONCLUSIONS

44 Based on our observations by combining HEXRD and MS measurements we propose that the
45 reduction under hydrogen of the carbon supported palladium sulphate precursor, PdSO₄-HHTox
46 sample, provides the Pd₄S based catalyst with superior selectivity to partial hydrogenation of
47 dialkenes. This approach supposes an easy and confident method to synthesize a well-defined
48 single palladium sulfide structure. Contrarily to Pd metal, where thermodynamically non-stable
49
50
51
52
53
54
55
56
57
58
59
60

1
2
3 surfaces and morphologies are required to obtain the desired selectivity, here we present a Pd₄S
4 phase with significant activity, appropriate selectivity and high stability under reaction
5 conditions. Moreover, an effect of particle size of the Pd₄S phase on the selectivity to partial
6 hydrogenation has been also observed, crystallites above 11 nm are likely needed for a full
7 selectivity to partial hydrogenation of butadiene. Finally we note that the experimental procedure
8 to obtain the sulfide phase is rather simple, non-requiring in-situ sulfidation steps.
9
10
11
12
13
14
15
16
17
18
19

20 ASSOCIATED CONTENT

21
22
23 **Supporting Information.** Figure S1 contains TPD–MS profiles of the HHTox and HHT-
24 SO₃H supports, Figures S2-S4 contain TEM micrographs of the different catalysts, Figures S5
25 and S6 contain additional HEXRD patterns for the catalysts and pure species, Figure S7 contains
26 XPS spectra of the S 2p region for the fresh PdSO₄-HHTox sample, Table S1 contains data
27 derived from application of Rietveld method to HEXRD patterns. This material is available free
28 of charge via the Internet at <http://pubs.acs.org>.
29
30
31
32
33
34
35
36
37
38
39

40 AUTHOR INFORMATION

41 42 43 **Corresponding Authors**

44
45
46 * irodriguez@icp.csic.es (I.R.-R.).
47
48

49
50 * aguerrero@ccia.uned.es (A.G.-R.).
51

52 53 **Funding Sources**

54
55 Ministerio de Economía y Competitividad (Spain). ESRF.
56
57
58
59
60

ACKNOWLEDGMENTS

We acknowledge financial support from the Spanish Ministerio de Economía y Competitividad (projects CTQ2011-29272-C04-01 and -03). The ESRF is thanked for granting beamtime at ID15.

REFERENCES

- 1 Bond, G. C. In *Metal-Catalysed Reactions of Hydrocarbons*, Springer, New York, 2005.
- 2 Bridier, B.; Karhánek, D.; Pérez-Ramírez, J.; López, N. *Chem. Cat. Chem.* **2012**, 4, 1420-1427.
- 3 McCue, A.J.; Anderson, J.A. *Catal. Sci. Technol.* **2014**, 4, 272-294.
- 4 McKenna, F.M.; Anderson, J.A. *J. Catal.* **2011**, 281, 231-240.
- 5 Cooper, A.; Bachiller-Baeza, B.; Anderson, J.A.; Rodríguez-Ramos, I.; Guerrero-Ruiz, A. *Catal. Sci. Technol.* **2014**, 4, 1446-1455.
- 6 Shao, L.; Zhang, W.; Armbüster, M.; Teschner, D.; Girgsdies, F.; Zhang, B.; Timpe, O.; Friedrich, M.; Schlögl, R.; Su, D.S. *Angew. Chem.* **2011**, 50, 10231-10235.
- 7 Silvestre-Albero, J.; Rupprechter, G.; Freund, H.J. *Chem. Commun.* **2006**, 80-82.
- 8 Zaera, F. *Chem. Sus. Chem.* **2013**, 6, 1797-1820.
- 9 Teschner, D.; Borsodi, J.; Wootsch, A.; Révay, Zs.; Havecker, M.; Knop-Gericke, A.; Jackson, S. D.; Schlögl, R. *Science* **2008**, 320, 86-89.

- 1
2
3 10 Xu, W.; Ni, J.; Zhang, Q.; Feng, F.; Xiang, Y.; Li, X. *J. Mater. Chem.* **2013**, 1, 12811-
4 12817.
5
6
7
8
9 11 Su, D.S.; Perathoner, S.; Centi, G. *Chem. Rev.* **2013**, 113, 5782-5816.
10
11
12 12 Serp, P.; Figueiredo, J.L. In *Carbon Materials for Catalysis*, John Wiley & Sons, Inc.,
13 New Jersey, 2009.
14
15
16
17 13 Zhang, Q.; Xu, W.; Li, X.; Jiang, D.; Xiang, Y.; Wang, J.; Cen, J.; Romano, S.; Ni, J.
18 *Appl. Catal. A: Gen.* **2015**, 497, 17-21.
19
20
21
22
23 14 Pang, S.H.; Schoenbaum, C.A.; Schwartz, D.K.; Medlin, J.W. *ACS Catal.* **2014**, 4, 3123-
24 3131.
25
26
27
28 15 Singh, V.V.; Kumar, U.; Tripathi, S.N.; Singh, A.K. *Dalton Trans.* **2014**, 43, 12555-
29 12563.
30
31
32
33
34 16 Ferri, D.; Newton, M.A.; Di Michiel, M.; Chiarello, G.L.; Yoon, S.; Lu, Y.; Andrieux, J.
35 *Angew. Chem. Int Ed.* **2014**, 53, 1-6.
36
37
38
39 17 Serp, P.; Corrias, M.; Kalck, P. *Appl. Catal. A: Gen.* **2003**, 253, 337-358.
40
41
42
43 18 Cuervo, M.R.; Asedegbega-Nieto, E.; Díaz, E.; Vega, A.; Ordóñez, S.; Castillejos-López,
44 E.; Rodríguez-Ramos I. *J. Chromatogr. A* **2008**, 1188, 264-273.
45
46
47
48 19 Almohalla, M.; Morales, M.V.; Asedegbega-Nieto, E.; Maroto-Valiente, A.; Bachiller-
49 Baeza, B.; Rodríguez-Ramos, I.; Guerrero-Ruiz, A. *TOCATJ* **2014**, 7, 1-7.
50
51
52
53
54 20 Bachiller-Baeza, B.; Peña-Bahamonde, J.; Castillejos, E.; Guerrero-Ruiz, A.; Rodríguez-
55 Ramos, I. *Catal. Today* **2015**, 249, 63-71.
56
57
58
59
60

- 1
2
3 21 Zlotea, C.; Cuevas, F.; Paul-Boncour, V.; Leroy, E.; Dibandjo, P.; Gadiou, R.; Vix-
4
5 Guterl, C.; Latroche, M. *J. Am. Chem. Soc.* **2010**, 132, 7720-7729.
6
7
8
9 22 JCPDS card no. 73-1387.
10
11
12 23 Hensen, E. J. M.; Brans, H. J. A.; Lardinois, G. M. H. J.; de Beer, V. H. J.; van Veen J.
13
14 A. R.; van Santen, R. *J. Catal.* **2000**, 192, 98–107.
15
16
17 24 Brun, M.; Berthet, A.; Bertolini, J.C. *J. Electron Spectrosc. Relat. Phenom.* **1999**, 104,
18
19 55-60.
20
21
22
23 25 Radha, B.; Kulkarni, G. U. *Adv. Funct. Mater.* **2010**, 20, 879–884.
24
25
26 26 Berhault, G.; Bisson, L.; Thomazeau, C.; Verdon, C.; Uzio, D. *Appl. Catal. A* **2007**, 327,
27
28 32-43.
29
30
31
32 27 Piccolo, L., Valcarcel, A.; Bausach, M.; Thomazeau, C.; Uzio, D.; Berhault, G. *Phys.*
33
34 *Chem. Chem. Phys.* **2008**, 10, 5504-5506.
35
36
37 28 Newton, M.A.; Di Michiel, M.; Kubacka, A.; Fernandez-Garcia, M. *J. Amer. Chem. Soc.*
38
39 **2010**, 132, 4540-4541.
40
41
42
43 29 Miller, J.B.; Alfonso, D.R.; Howard, B.H.; O'Brien, C.P.; Morreale, B.D. *J. Phys. Chem.*
44
45 *C* **2009**, 113, 18800-18806.
46
47
48
49 30 O'Brien, C.P.; Gellman, A.J.; Morreale, B.D.; Miller, J.B. *J. Membr. Sci.* **2011**, 371, 263-
50
51 267.
52
53
54 31 Diaz-Chao, P.; Ferrer, I.J.; Ares, J.R.; Sanchez, C. *J. Phys. Chem. C* **2009**, 113, 5329-
55
56 5335.
57
58
59
60

Table of Contents Graphic and Synopsis

Hard X-ray diffraction coupled with mass spectrometry enabled to find out a simple method to synthesize a catalyst based on palladium sulphide (Pd_4S) nanoparticles supported on carbon which has significant activity, appropriate selectivity and high stability under reaction conditions of 1,3-butadiene hydrogenation.

